R. L. Jones and J. R. Gordon†*

The Effect of Specimen Size and Geometry on *J–R* Curve Behaviour

REFERENCE Jones, R. L. and Gordon, J. R., **The effect of specimen size and geometry on *J–R* curve behaviour**, *Defect Assessment in Components – Fundamentals and Applications*, ESIS/EGF9 (Edited by J. G. Blauel and K.-H. Schwalbe) 1991, Mechanical Engineering Publications, London, pp. 271–284.

ABSTRACT This paper presents results from an experimental programme to study geometry and size effects in *J–R* curves. The results presented were obtained at room temperature from unloading compliance *R* curve tests on different sized single edge notch bend specimens of HY100 steel.

The crack growth resistance was measured in terms of the standard fracture resistance, *J*, *J*-corrected for crack growth and the *J*-modified parameter proposed by Ernst.

It was found that the limit to *J*-controlled crack growth was best described by the J_M parameter and that apparent size independence seen from J_0 and J_R *R* curves at larger crack extensions is purely coincidental.

Notation

a	Crack length
a_0	Initial crack length
Δ_a	Crack extension
B	Specimen thickness
B_n	Net thickness
b	Uncracked ligament
E	Young's modulus
J	Fracture resistance J
J_R	J-corrected for crack growth
J_M	Modified J
S	Loading span
W	Specimen width
ρ, α, ω	Parameters for specifying the limits of J-controlled crack growth
σ_{YS}	Yield strength
σ_{flow}	Flow strength
Δ	Load point displacement
MOD	Mouth opening displacement

Introduction

When a material exhibits fully ductile behaviour its resistance to crack extension is usually presented in the form of an elastic–plastic crack growth resistance curve (*R* curve). In essence the *R* curve is a plot of the variation in crack

* Admirality Research Establishment, Holton Heath, Poole, Dorset, UK.
† Edison Welding Institute, Columbus, Ohio, USA.

growth resistance, generally expressed in terms of CTOD or J, during the process of stable crack extension.

Over the last few years recommended test procedures have been published **(1)–(5)** which cover the measurement of J–R curves using either the well established multiple specimen method or the single specimen unloading compliance technique. Provided certain restrictions are satisfied the resulting R curves can be regarded as material properties. The purpose of the limitations is to ensure that J remains a valid characterising parameter during the process of stable crack extension. If these conditions are satisfied the crack growth process is frequently referred to as being J-controlled.

The first restriction for J-controlled crack growth relates to the minimum specimen size required to produce plane strain constraint and ensure J-dominance **(4)**. This limitation is usually presented in the form

$$B, b > \rho \frac{J}{\sigma_{\text{flow}}}, \rho = 25 \text{ for bend and compact geometries} \quad (1)$$

where B = specimen thickness
b = the uncracked ligament and
σ_{flow} = the material's flow strength (usually taken as the average of the yield and tensile strengths).

In addition to the above specimen size requirements there are two further limitations which apply to J to ensure 'J-controlled crack growth'. These restrictions, which are based on theoretical considerations, arise from the fact that J is only strictly valid for stationary cracks. However, provided the crack extension is limited to a small proportion of the ligament, equation (2), and that J increases sufficiently rapidly with crack growth so that J-characterised proportional loading occurs, equation (3), then J can be considered as a characterising parameter which controls crack growth.

$$\Delta a \leqslant \alpha(W - a_0) \quad (2)$$

$$\omega = \frac{b}{J}\frac{\text{d}J}{\text{d}a}, \omega \gg 1.0 \quad (3)$$

where W = specimen width
a_0 = initial crack length.

A number of numerical and experimental studies have been undertaken to determine the limiting values of α and ω for different specimen geometries. For bend specimens it has been proposed that the limiting value of α lies in the range 0.06–0.1 **(4)–(6)**, whilst ω should exceed either 2.5 **(5)** or 10.0 **(4)**.

This paper presents results of part of a large experimental programme to study the effects of specimen geometry and size on elastic–plastic crack growth resistance curves and, in particular, determine the limits of J-controlled crack growth. The test programme includes low, medium, and high toughness materials. Preliminary results have been published from a low toughness titanium alloy **(7)**. This paper gives results from an HY100 steel.

The crack growth resistance is measured in terms of the following fracture toughness parameters.

(1) Standard fracture resistance J (i.e., uncorrected for crack growth) (J_0).
(2) J-corrected for crack growth (J_R).
(3) Ernst modified J (J_M) **(8)**.

Material

The material selected for this investigation was HY100 grade steel in the form of a 75 mm thick plate. The high tearing resistance alloy has a nominal yield strength of 875 N/mm^2 and a tensile strength of 910 N/mm^2.

The material was supplied in the quench and tempered condition. A macro section showed no evidence of segregation through the thickness. This was also demonstrated from a preliminary assessment of through thickness fracture properties, where three specimens taken from top, middle, and bottom locations were shown to demonstrate essentially similar J–Δ_a R curve behaviour.

Test programme

General

The test programme consisted of 27 room temperature, unloading compliance R curve tests on single edge notch bend (SENB) specimens of different sizes. The SENB specimens, which were all in the L–T orientation with respect to the rolling direction of the plate, were sidegrooved by 20 percent after being fatigue pre-cracked to provide initial crack length to specimen width ratios (a_0/W) of approximately 0.6.

All the SENB specimens were tested with a loading span to specimen width ratio (S/W) of 4.0.

'Size effects' programme

Five SENB specimen sizes were studied in this programme corresponding to nominal thicknesses of 15, 30, 45, 60, and 75 mm. All the specimens have a thickness equal to half the width ($B \times 2B$). For each specimen size three room temperature unloading compliance tests were performed. Details of the specimens are given in Table 1.

'Geometry effects' programme

Five SENB specimen geometries were studied in this programme corresponding to $B \times \frac{1}{2}B$, $B \times B$, $B \times 2B$, $B \times 3B$, and $B \times 4B$. All the specimens had a nominal thickness (B) of 30 mm. For each specimen geometry three room temperature, unloading compliance tests were performed. Details of the specimens are also given in Table 1.

Table 1 Details of SENB specimens

Specimen numbers	*Specimen dimensions* Thickness, B (mm)	Width, W (mm)	*Net Thickness, B_n (mm)*
	(a) *Size Effects Programme*		
1–3	15	30	12
4–6	30	60	24
7–9	45	90	36
10–12	60	120	48
13–15	75	150	60
	(b) *Geometry Effects Programme*		
16–18	30	15	24
19–21	30	30	24
4–6	30	60	24
22–24	30	90	24
25–27	30	120	24

Test details

The specimens were tested in broad agreement with the ASTM recommended *R* curve procedure **(3)** using a computerised unloading compliance test system employing a data acquisition unit.

During the tests, time, applied load, upper and lower clip gauge displacement, and ram displacement were continually measured. The load point displacement was determined by correcting the measured ram displacement for extraneous displacements arising from test machine and fixture compliance, and roller indentation effects **(1)**. Further details of the test procedure are given in reference **(7)**.

The crack length at each unloading was estimated using the following compliance relationship

$$a/W = 0.999748 - 3.9504\mu + 2.9821\mu^2 - 3.21408\mu^3 + 51.51564\mu^4 - 113.031\mu^5 \quad (4)$$

$$\text{where } \mu = \frac{1}{\left[\dfrac{4WEB_{\text{eff}}}{S} C_{\text{orr}}\right]^{1/2} + 1} \quad (5)$$

$$B_{\text{eff}} = B - (B - B_n)^2/B \quad (6)$$

E = Young's modulus

$$\text{and } C_{\text{orr}} = \frac{C_{\text{measured}}}{FD}$$

The compliance correction factor FD has been proposed **(9)** to quantify the deviation of the compliance of the deformed SENB specimen from its theoretical value and is given by

$$D = 1 - 0.665 \frac{\Delta}{2W} \quad (7)$$

Values of J_0, J_R, and J_M were also calculated at each unloading for the condition immediately before the 5 percent unloading.

The unloading compliance tests were terminated after the crack had grown by approximately 50 percent of the original uncracked ligament. On completion of the tests the specimens were heat tinted before being cooled down to −196°C and broken open. Both the initial fatigue crack length (a_0) and the stable crack growth (including stretch zone) were calculated using the weighted nine point average method **(1)**.

All the unloading compliance tests satisfied the requirement that the measured and predicted crack growth should not differ by more than 10 percent.

Standard fracture resistance J *(J_0)* In the case of a sidegrooved SENB specimen the standard fracture resistance J (i.e., uncorrected for crack growth) can be calculated using the following expression

$$J_0 = \frac{2U}{B_n(W - a_0)} \quad (8)$$

where U = area under load versus load point displacement record.

J-*corrected for crack growth (J_R)* The above expression for J_0 is based on initial crack length and therefore does not take account of crack growth during a test. If necessary J can be corrected for crack growth using the following expression proposed by Ernst:

$$J_{R_k} = \left\{J_{R_{k-1}} + \left(\frac{2}{b}\right)_{k-1}\left(\frac{U_{k-1\cdot k}}{B_n}\right)\right\}\left\{1 - \left(\frac{1}{b}\right)_{k-1}(a_k - a_{k-1})\right\} \quad (9)$$

where J_{R_k} = J_R evaluated at crack length a_k
$U_{k-1,k}$ = the increment of area under the load versus load point displacement record between lines of constant displacement at unloading $k-1$ and k
a_k = crack length at kth loading
b_k = $W - a_k$

J-*modified (J_M)* In an attempt to extend the range over which J can be applied Ernst **(8)** has proposed a modified version of J denoted J_M. This parameter is given by the expression

$$J_M = J_R + \int_{a_0}^{a} \frac{\partial(J_{pl})}{\partial_a}\bigg|_{\Delta_{pl}} da \quad (10)$$

where J_{pl} = plastic component of J_R
Δ_{pl} = plastic component of load displacement

In the case of a sidegrooved SENB specimen J_M can be calculated using the following incremental expression

$$J_{M_k} = J_{M_{k-1}} + (J_{R_k} - J_{R_{k-1}}) + J_{pl_{k-1}}\left(\frac{1}{b_{k-1}}\right)(a_k - a_{k-1}) \tag{11}$$

where $J_{pl_{k-1}}$ = plastic component of J_R at unloading $k - 1$.

Results

Size effects programme

The mean J_0–R curves obtained for each specimen size are compared in Fig. 1. This shows that after a period of initial agreement the larger specimens have shallower gradients than those obtained from smaller specimens. The crack growth limit for the 75 × 150 mm specimen is included in the figure. As may be seen, the curve for the 45 × 90 mm specimen is coincident with the 75 × 150 mm curve up to this limit. The 60 × 120 mm curve lies slightly above the 75 × 150 mm curve and runs parallel to it for most of its length. The observed offset is probably associated with material variability. The 15 × 30 mm and 30 × 60 mm curves form an upper bound and are themselves coincident.

The mean J_R–R curves are compared in Fig. 2. As shown there is good agreement for the three largest specimen sizes over the full length of the

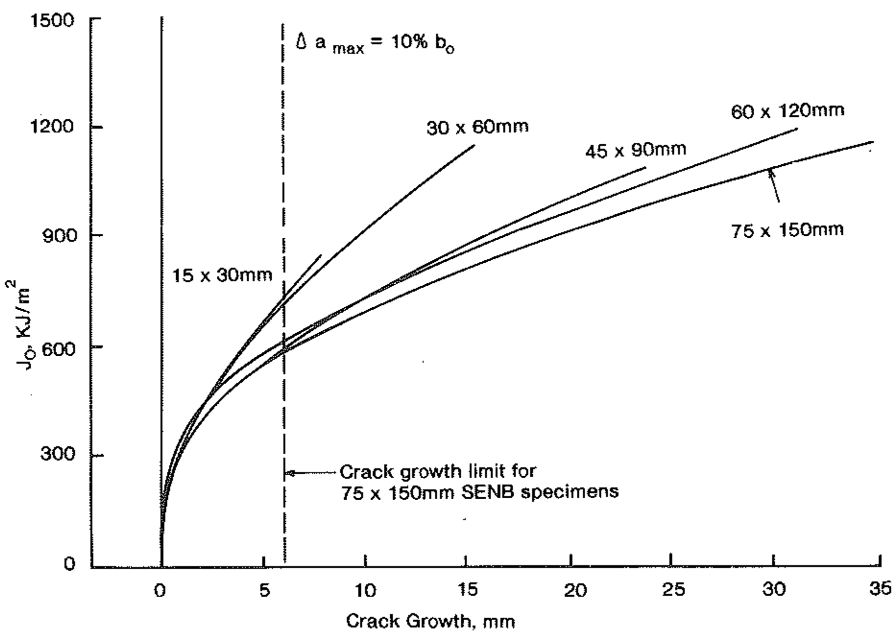

Fig 1 Comparison of J_0–R curves (size effects programme)

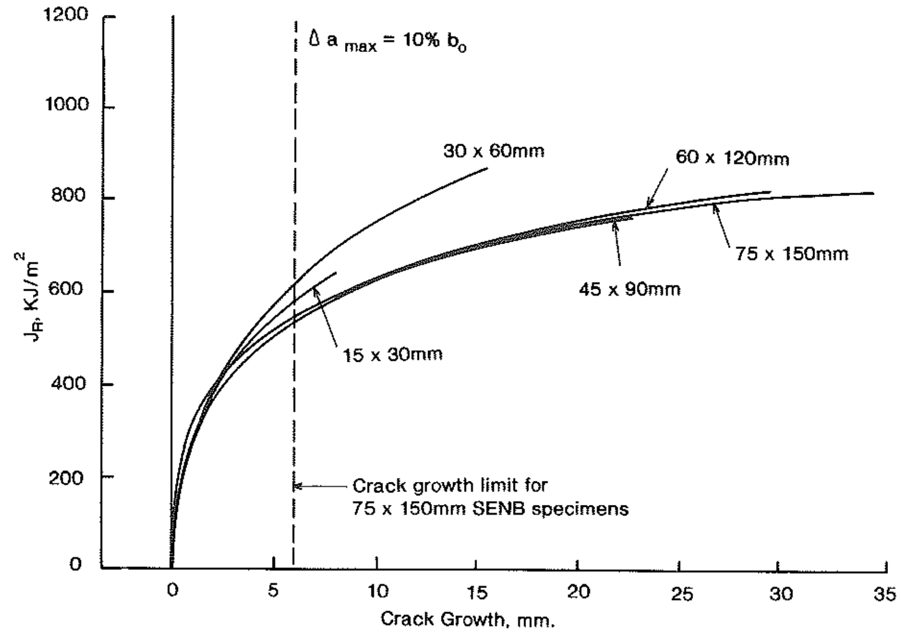

Fig 2 Comparison of J_r–R curves (size effects programme)

curves. The two smaller specimen sizes again are an upper bound, however, in comparison to the J_0 curves the 15 × 30 mm specimen deviates from the 30 × 60 mm specimen at a smaller amount of crack growth.

The mean J_M–R curves are compared in Fig. 3. The behaviour of these curves is different from the J_0 and J_R behaviour, in that following an initial period of agreement the curves split and show a shallow uprising.

Geometry effects programme

The main J–R curves for J_0, J_R, and J_M obtained from the geometry effects study are summarised in Figs 4, 5, and 6. Also included in these figures is the R curve and crack growth limit for the 75 × 150 mm size specimen.

As shown in Fig. 4, shallower gradient curves are obtained for J_0 for the increasing width specimens. The 60 and 90 mm width specimens form a common curve with the 120 mm specimen up to and just beyond the crack growth limit for the 75 × 150 mm specimen. The two smaller width specimens are seen to 'peel off' the larger width specimen curves after crack growth of less than 1 mm. As shown, all the geometry effects specimen curves lie above the 75 × 150 mm reference curve.

The main J_R curves are given in Fig. 5. As shown, similar trends are observed to the J_0 curves although in this instance the level of agreement between the curves is extended to greater amounts of crack growth.

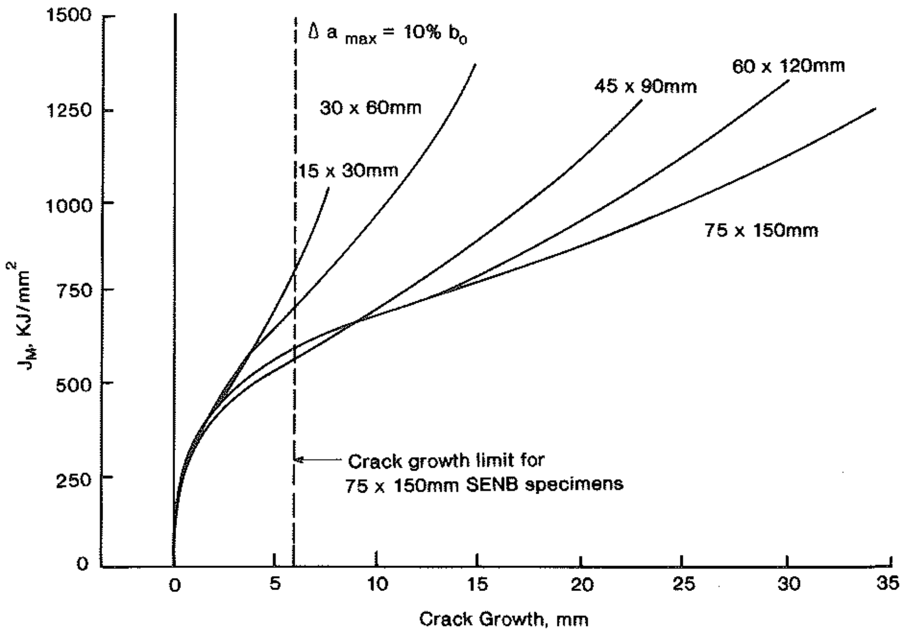

Fig 3 Comparison of J_m–R curves (size effects programme)

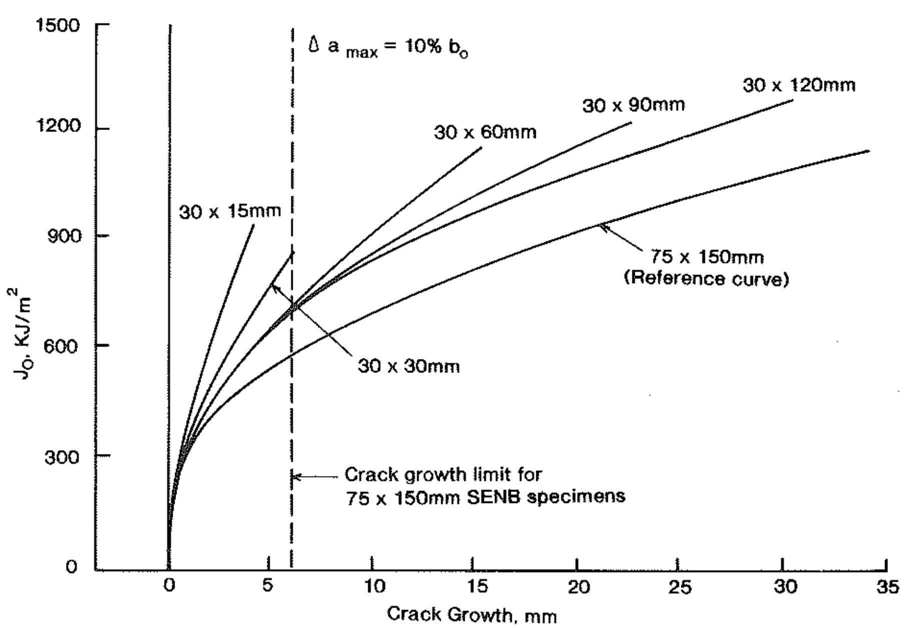

Fig 4 Comparison of J_0–R curves (geometry effects programme)

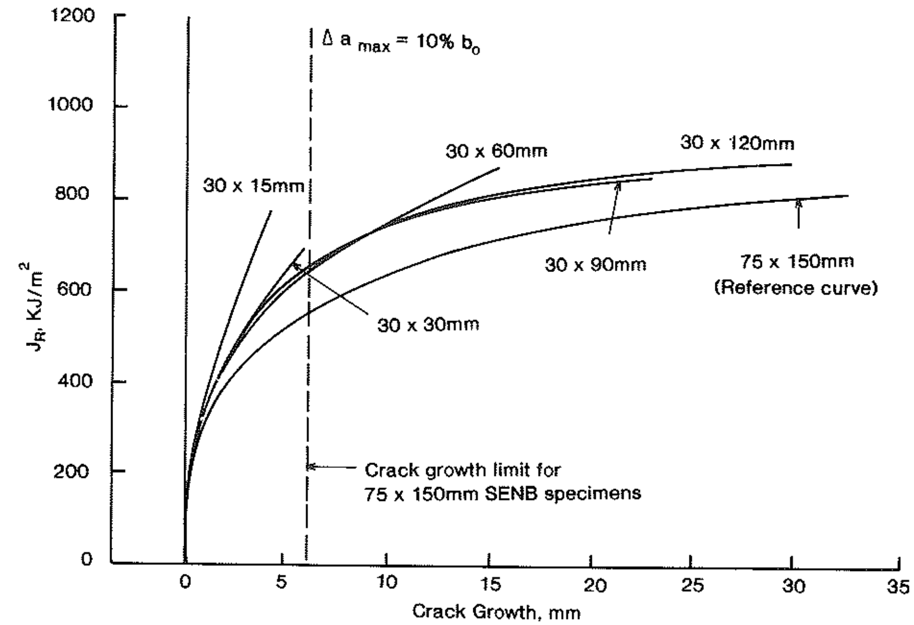

Fig 5 Comparison of J_r–R curves (geometry effects programme)

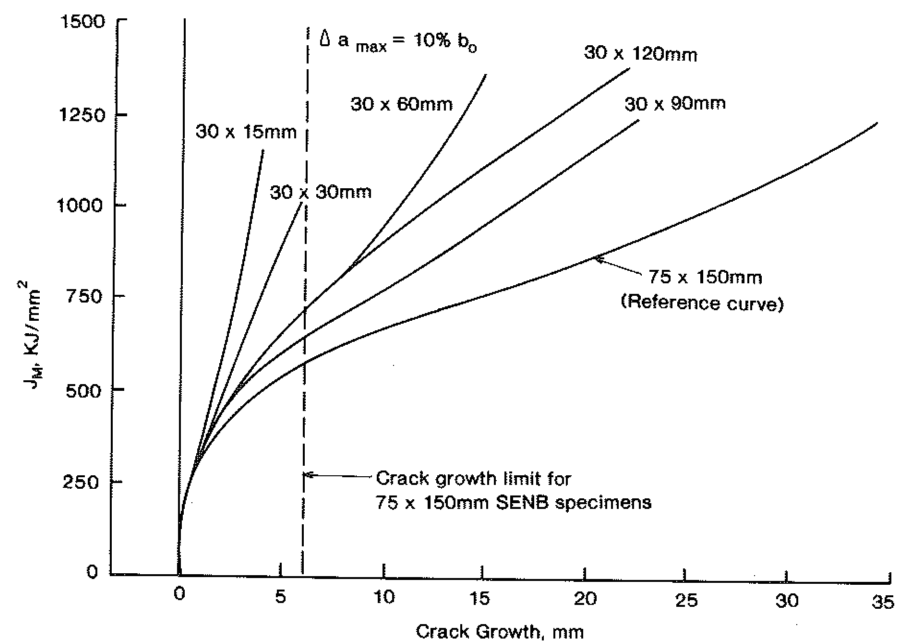

Fig 6 Comparison of J_m–R curves (geometry effects programme)

The J_M–R curves for the geometry effects programme are compared in Fig. 6. Similar to the size effects study it is seen that following initial agreement the curves diverge and show a gentle upswing.

Discussion of results

At the onset of the programme it had been considered that the limits of J-controlled crack growth would be determined by identifying the point at which the small specimen R curves separated from the 75 × 150 mm reference curve. However, as demonstrated from the previous work on a titanium alloy the breakdown of J-controlled crack growth is a gradual process which is complicated by material variability and, consequently, the R curves do not exhibit well defined separation points.

From the size effects study it is shown that, irrespective of the method of calculating J, the two smaller specimen size curves depart from the reference curve following approximately 3 mm of crack extension, whilst the larger specimen curves appear to follow the reference curve for greatly extended amounts of crack extension. From these observations it would appear that specimen constraint is the limiting factor. It is considered that the limit of J-control crack growth may be depicted from the breakdown of constraint observed from a plot of specimen bend against crack extension.

Plots of specimen bend versus crack extension were obtained from both load point displacement (LPD) and the mouth opening displacement (MOD) records. In the first instance LPD was normalised by specimen span and in the second instance by the initial ligament length. Since the trends shown were similar, only the data obtained from the MOD is presented. Plots of normalised MOD versus crack extension normalised by initial ligament are given for the size and geometry effects studies in Figs 7 and 8, respectively.

As shown, there is an initial rapid increase in normalised MOD with normalised crack extension followed by a region of linear dependence. Eventually the curves show an upswing denoting that an increasing amount of specimen bend is required to cause additional crack extension. The slope of the linear part of the curve is a function of specimen size and geometry. Shallower gradients being seen for increasing specimen size and increasing W dimension. It is noted that the curves are closer together for the larger specimen sizes and appear to approach a limiting value. It is postulated that the limit to J-controlled crack growth occurs at the upswing in the curve. However, the slope of the linear portion of the curve may also indicate the level of constraint and some minimum value may also have to be met in order to satisfy the conditions for plane strain constraint.

From Fig. 7 for the size effects tests it is estimated that the crack extension factor α ranges from 0.2 for $W = 30$–0.32 for $W = 150$ mm. From Fig. 8 for the geometry effects tests it is similarly estimated that α ranges from 0.24 for $W = 15$ raising to 0.30 for $W = 120$ mm. The data given in Figs 7 and 8 are

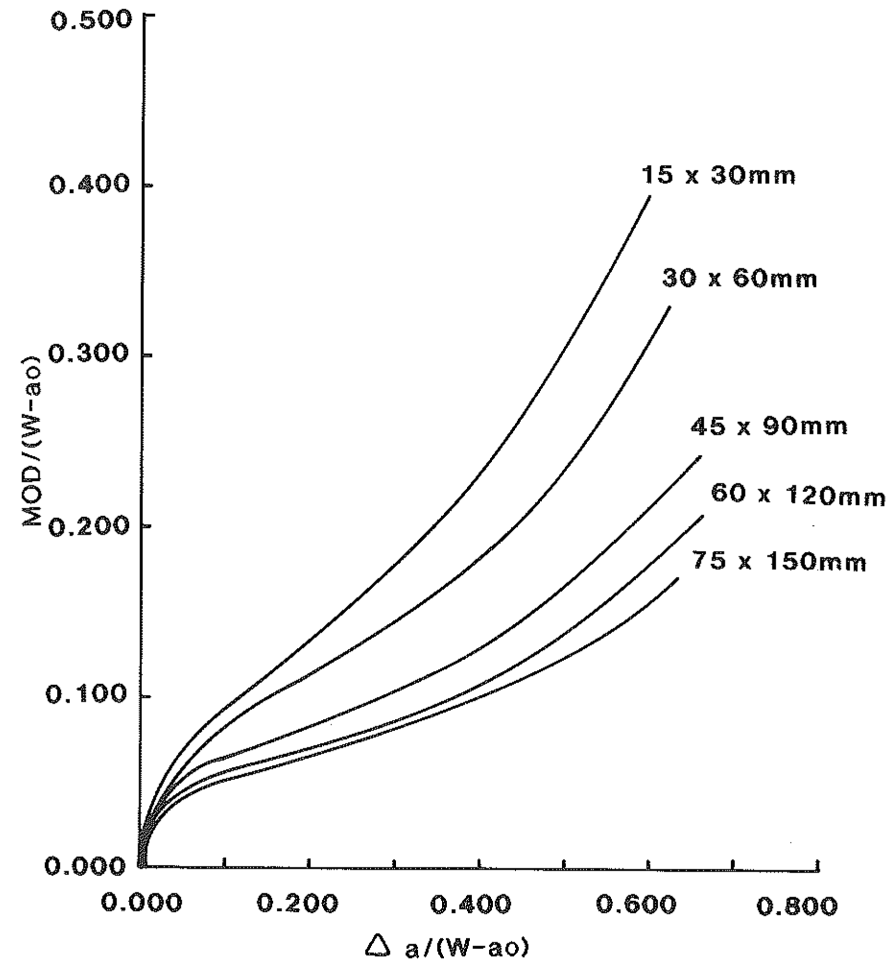

Fig 7 Normalised mouth opening displacement against normalised crack extension (size effects programme)

for specific tests and therefore direct comparison with the breakdown in agreement between mean R curve behaviour given in Figs 1–6 is not possible. However, as shown in Table 2 the crack extensions corresponding to the upswing in the normalised MOD curves are similar to the crack extensions observed in the upswing of the mean J_M curves.

It is therefore considered that the point of upswing in the J_M curves also defines the limit to J-controlled crack growth and that apparent size independence in J–R curve behaviour seen at larger crack extensions seen from J_0 and J_R–R curves is purely coincidental.

Values of α, ρ, and ω at the point of upswing in the J_M–R curves are given in Table 3.

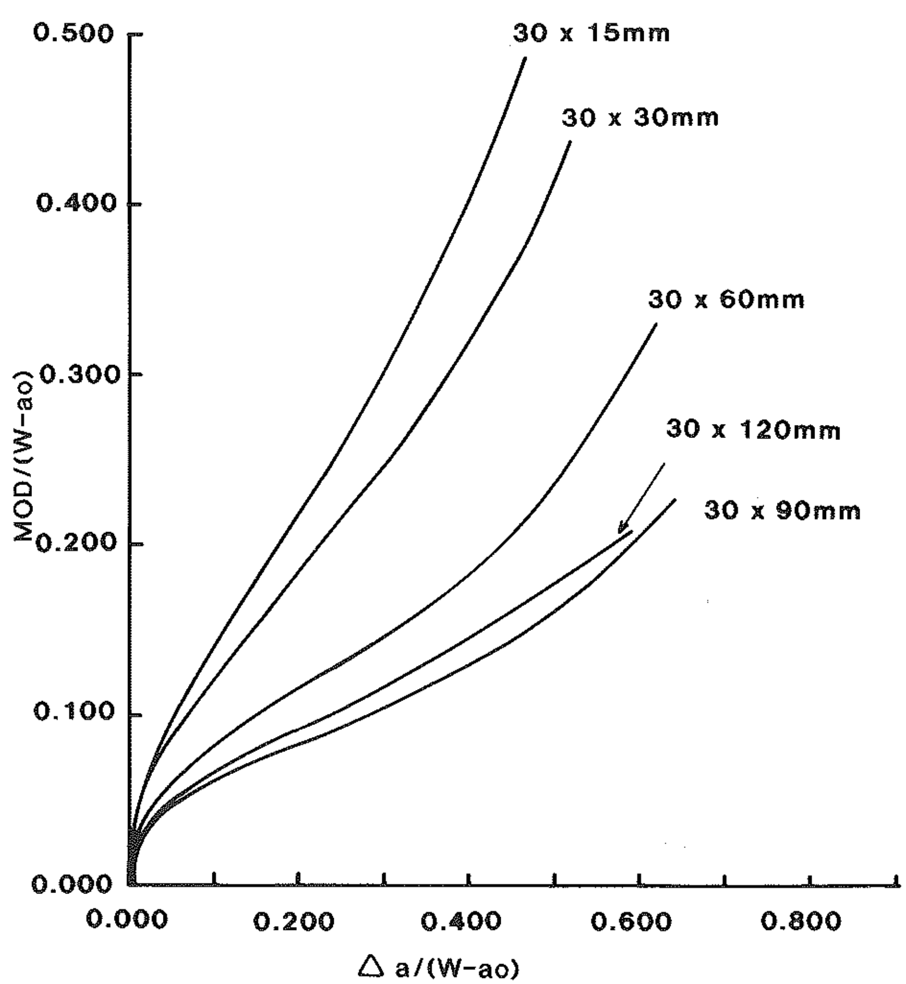

Fig 8 Normalised mouth opening displacement against normalised crack extension (geometry effects programme)

As seen, the limiting value of the crack extension factor α is given as 0.22 compared to normally accepted upper limit of 0.1.

It is of note that for the size effects study the $W = 90$, 120, and 150 mm J_m–Δa data can be considered to form a common curve up to their points of upswing, whilst the two smaller specimen sizes, $W = 30$ and 60 mm, depart from this common curve at an earlier stage. For the $W = 30$ and 60 mm specimens the ρ factor at upswing is given in Table 3 as 16.5 and 197.7 compared to values of 37.6, 39.0, and 43.5 for the larger specimens. It would, therefore, appear that for the two smaller size specimens the ρ factor is controlling the J–Δa behaviour and that a minimum value of 25, as is normally accepted, is required to ensure plane strain constraint.

Table 2 Comparison of point of upswing in specimen bend and J_m curves

	Specimen no.	W	b_0	Point of upswing in Figs 7 and 8: Δa / $(\omega - a_0)$	Point of upswing in Figs 7 and 8: Δ_a	Point of upswing in J_m curve: Δ_a
Size effects	M04-03	30.02	12.81	0.200	2.56	2.86
	M04-04	60.13	24.29	0.236	5.73	6.73
	M04-08	90.04	35.41	0.253	8.97	7.87
	M04-12	120.24	46.69	0.293	13.68	13.05
	M04-14	147.14	56.74	0.32	18.15	16.36
Geometry effects	M04-16	15.05	7.56	0.24	1.81	1.86
	M04-19	30.01	11.51	0.24	2.76	>6.2
	M04-04	60.13	24.29	0.24	5.83	6.73
	M0422	90.02	35.71	0.30	10.89	11.4
	M04-25	120.11	48.48	0.30	14.54	>22.15

As shown in Fig. 6 the J_M–R curves show geometry independence for only limited amounts of crack extension. A comparison of the data given in Table 3 shows that apart from one exception the ρ factor at upswing is less than 25 and that therefore conditions of plain strain constraint do not apply.

The ω parameter does not appear to be a limiting factor. It is, however, indicated from these studies that this parameter may be relaxed to a value of 1.0.

From the results of this work it is postulated that the limit to J-controlled crack growth may be ascertained from either the point of upswing in normalised MOD versus normalised crack extension curve or from the point of upswing in the J_M–R curve. For HY100 steel this limit to J-controlled crack growth is equivalent to a crack extension factor of 0.2.

This condition alone is, however, not sufficient to ensure size/geometry independent J–R curves. To achieve size/geometry independence it is necessary to have the same level of specimen constraint. This is most readily achieved by

Table 3 Values of α, ρ and ω at point of upswing in J_M–R curves

Specimen size	*Δ_a at sep*	α	ρ	ω
15 × 30	2.86 mm	0.22	16.5	1.8
30 × 60	6.73 mm	0.28	19.7	1.4
45 × 90	7.87 mm	0.22	37.6	1.5
60 × 120	13.05 mm	0.28	39.0	1.0
75 × 150	16.36 mm	0.29	43.5	1.0
30 × 15	1.86 mm	0.25	8.7	2.1
30 × 30	>6.21 mm (No upswing)	0.54	4.6	0.7
30 × 60	6.73 mm	0.28	19.7	1.3
30 × 90	11.4 mm	0.31	28.3	1.5
30 × 120	22.15 mm (No upswing)	0.46	16.3	0.7

ensuring that plane strain conditions apply, namely by maintaining a ρ factor in excess of 25.

Conclusions

An indication of specimen constraint is shown from a plot of normalised MOD against normalised crack extension.

The limit of J-controlled crack growth may be defined as the point of upswing in the normalised MOD versus normalised crack extension curve, this being equivalent to the point of upswing in the J_M–R curves.

Limiting values of $\alpha = 0.2$, $\rho = 25$, and $\omega = 1.0$ are required to ensure size/geometry independence for HY100 steel.

References

(1) GORDON, J. R. (1985) The welding institute procedure for the determination of the fracture resistance of fully ductile metals, *Weld. Inst. Res. Rep.*, **275**.
(2) NEALE, B. K., CURRY, D. A., GREENE, G., HAIGH, J. R., and AKHURST, K. N. (1984) A procedure for the determination of the fracture resistance of ductile steels, *Int. J. Press. Vess. Piping*, **20**, 155–179.
(3) ASTM E1152 (1987) Standard method for determining *J–R* curves.
(4) SHIH, C. F. and GERMAN, M. D. (1981) Requirements for a one parameter characterisation of crack tip fields by the HRR-singularity, *Int. J. Fract.*, **17**, 27–43.
(5) LANDES, J. D. (1979) Size and geometry effects on elastic–plastic fracture characterisation, CSNI Specialists Meeting on Plastic Tearing Instability, *NUREG/CP*-**0010**, 194–225.
(6) HUTCHINSON, J. W. (1983) Fundamentals of the phenomenological theory of non-linear fracture mechanics, *J. Appl. Mech.*, **50**, 1042–1051.
(7) GORDON, J. R. and JONES, R. L. (1989) The effect of specimen size on the *J–R* curve behaviour of a titanium alloy, *Fatigue Fract. Engng Mater. Struct.*, **12**, **4**, 295–308.
(8) ERNST, H. A. (1983) Material resistance and instability beyond *J*-controlled crack growth, elastic–plastic fracture, *ASTM STP* **803**, **I**, 191–213.
(9) STEENKAMP, P. A. J. M. (1986) Investigation into the validity of *J*-based methods for the prediction of ductile tearing and fracture, *PhD Thesis*, Delft University, Holland.